

# Experimental evaluation of an Internal Heat Exchanger in a CO<sub>2</sub> subcritical refrigeration cycle with gas-cooler.

**Rodrigo Llopis<sup>1,\*</sup>, Carlos Sanz-Kock<sup>1</sup>, Ramón Cabello<sup>1</sup>, Daniel Sánchez<sup>1</sup>, Enrique Torrella<sup>2</sup>**

*<sup>1</sup>Jaume I University, Dep. of Mechanical Engineering and Construction, Campus de Riu Sec s/n  
E-12071, Castellón, Spain*

*<sup>2</sup>Polytechnic University of Valencia, Department of Applied Thermodynamics, Camino de Vera, 14,  
E-46022, Valencia, Spain*

\*Corresponding author: R. Llopis ([rllopis@uji.es](mailto:rllopis@uji.es)), Phone: +34 964 72 8136; Fax: +34 964 728106.

## ABSTRACT

We present the experimental evaluation of an internal heat exchanger or suction-line/liquid-line heat exchanger in a CO<sub>2</sub> subcritical refrigeration plant with gas-cooler. The plant, driven by a 1.5kW CO<sub>2</sub> semi hermetic compressor, uses brazed plate heat exchangers as condenser, evaporator and internal heat exchanger, an air finned tube gas-cooler and an electronic expansion valves. The evaluation (77 steady-states) covers evaporating temperatures from -40 to -25 °C and condensing temperatures from -15 to 0 °C, always at the nominal speed of the compressor. Here, the effect of the internal heat exchanger on the main energy parameters is analysed, i.e., cooling capacity, COP and heat rejection at gas-cooler and condenser. Also, the effect of the internal heat exchanger in a cascade cycle is analysed theoretically. It has been concluded that the internal heat exchanger does not improve the performance of the subcritical cycle, but it could improve the energy performance if it is used inside a cascade refrigeration system.

## KEYWORDS

CO<sub>2</sub>; subcritical; internal heat exchanger; cascade; experimental

## NOMENCLATURE

---

$COP$	coefficient of performance
$c_p$	specific isobaric heat, $\text{kJ}\cdot\text{kg}^{-1}\cdot\text{K}^{-1}$
$h$	specific enthalpy, $\text{kJ}\cdot\text{kg}^{-1}$
$\dot{m}_r$	$\text{CO}_2$ refrigerant mass flow rate, $\text{kg}\cdot\text{s}^{-1}$
$\dot{m}_{r,HT}$	R134a refrigerant mass flow rate, $\text{kg}\cdot\text{s}^{-1}$
$P$	pressure, bar ; power consumption, kW
$q_o$	specific cooling capacity, $\text{kJ}\cdot\text{kg}^{-1}$
$\dot{Q}$	heat transfer rate, kW
SH	superheating degree, $^{\circ}\text{C}$
SUB	subcooling degree, $^{\circ}\text{C}$
$T$	temperature, $^{\circ}\text{C}$
$\dot{V}_g$	secondary volumetric flow rate in evaporator, $\text{m}^3\cdot\text{s}^{-1}$
$\dot{V}_G$	compressor displacement, $\text{m}^3\cdot\text{s}^{-1}$

## GREEK SYMBOLS

---

$\rho$	density, $\text{kg}\cdot\text{m}^{-3}$
$\varepsilon$	thermal effectiveness
$\eta_v$	volumetric efficiency of the compressor
$\Delta$	increment
$v$	specific volume, $\text{m}^3\cdot\text{kg}^{-1}$

## SUBSCRIPTS

---

C	compressor
<i>casc</i>	referred to a cascade system
<i>g</i>	secondary fluid in evaporator
<i>gc</i>	gas cooler
<i>HT</i>	high temperature cycle
<i>i</i>	inlet
<i>IHX</i>	internal heat exchanger
<i>K</i>	condenser
<i>l</i>	liquid

<i>o</i>	outlet
<i>O</i>	evaporator
<i>r</i>	refrigerant CO <sub>2</sub>
<i>suc</i>	compressor inlet
<i>v</i>	vapour

## 1. Introduction

---

The Internal Heat Exchanger (IHX) or suction/liquid heat exchanger is generally used in refrigeration plants to ensure a proper function of the system and protect the integrity of the components. Its use avoids the risk of flashing gas at the inlet of the expansion device caused by pressure losses or heat transfer, since with the IHX the expansion device is fed with subcooled liquid. In addition, the IHX reduces the possibility of liquid entering to the compressor suction, as if liquid is present at the exit of the evaporator, it is evaporated in this heat exchanger. The IHX causes an increase on the specific suction volume, on the discharge temperature, a reduction of the refrigerant mass flow rate, an increase of the specific cooling capacity and pressure losses. But from the point of view of energy efficiency (COP), its effect can be positive or negative, depending on the considered refrigerant [1]. Using a theoretical approach and neglecting pressure drop, Domanski et al. [2] concluded that it is beneficial for refrigerants with high heat capacity. Mastrullo et al. [3], considering pressure losses, obtained similar conclusions about the heat capacity, but they added that the IHX is more recommended for refrigerants that provide low COP.

The IHX is optional for plants working at high evaporating temperatures, but its use is highly recommended for applications at low evaporating temperatures, those evaporating below  $-20^{\circ}\text{C}$ , approximately. In fact, compressors manufacturers recommend to operate the plants with a minimum gas superheat at suction of 20 K to avoid problems related with lubrication and to extend the useful life of the compressor. To achieve it two possibilities exist, increasing the degree of superheat at the evaporator with the expansion device, which turns usually in a decrease of energy efficiency, or using the IHX, which influence on the energy efficiency will depend on the considered refrigerant.

After the adoption of the new F-Gas regulation in Europe [4], the systems which are attracting more attention for commercial refrigeration at low evaporating temperatures are cascade plants using  $\text{CO}_2$  as low temperature refrigerant [5, 6], which operate with an evaporating temperature of  $-30^{\circ}\text{C}$  or below. For this system, the use of the IHX is recommended, however, to the knowledge of the authors no results have been published in literature about its energy performance in  $\text{CO}_2$  subcritical cycles at this operating conditions. The only results available are the ones presented by Zhang et al. [7], who evaluated theoretically the effects of the IHX in a single-stage subcritical  $\text{CO}_2$  refrigeration plant for evaporating temperatures from  $-20$  to  $-10^{\circ}\text{C}$  with condensing temperatures from  $10$  to  $20^{\circ}\text{C}$ . They observed COP was slightly reduced by the use of the IHX in subcritical operation, but they pointed out it is convenient for transcritical operation. About the use of the IHX in transcritical plants some experimental research has been published. Torrella et al. [8] for evaporating temperatures from  $-15$  to  $-5^{\circ}\text{C}$  and gas-cooler outlet temperatures from  $31$  to  $34^{\circ}\text{C}$  verified experimentally that the IHX enhanced the energy performance. They measured increments of COP and cooling capacity up to 12%, and observed the improvement was better at low evaporating temperatures. Also, Sanchez et al. [9], under a different experimental analysis

and with different locations of the IHX in the transcritical cycle, observed it improved the performance. The unique drawback pointed out by the authors was the increase of the compressor discharge temperature due to the use of the IHX, which reached up to 20°C.

As mentioned, the influence of the IHX in CO<sub>2</sub> subcritical cycles has only been addressed theoretically for operating conditions over -20 °C of evaporating temperature and for condensing temperature higher than 10 °C [7]. Also, the usual criterion to determine the possible advantage of adopting this heat exchanger (Domanski et al. [2], Aprea et al. [10] and Klein et al. [11]) do not offer coherent results for subcritical CO<sub>2</sub> cycles, since the condensing temperatures of the CO<sub>2</sub> subcritical cycles are lowest than the considered for establishing the criterions. Accordingly, the objective of this work is to cover this lack of research presenting the experimental evaluation of the energy implications of the use of the IHX in a CO<sub>2</sub> subcritical refrigeration plant for low evaporating temperatures and discussing its energy implication. The evaluation, made with an experimental plant driven by a semi hermetic compressor, covers evaporating temperatures from -40 to -25 °C and condensing temperatures from -15 to 0 °C, the usual temperature range in commercial refrigeration at low temperature.

## **2. Experimental plant and measurement system**

---

The results analysed in this work are based on the experimental results obtained with an experimental CO<sub>2</sub> subcritical refrigeration plant whose scheme is presented in Figure 1. The plant is driven by a CO<sub>2</sub> semi hermetic compressor for subcritical applications, with a displacement of 3.48 m<sup>3</sup>/h at 1450 rpm and a nominal power of 1.5 kW that is controlled by an inverter. The used lubricant oil is POE C55E. The compressor absorbs the vapour at suction (point 1) and compresses it to the high pressure (point 2), then the lubricant oil is separated. Following, the refrigerant gets into a gas-cooler (point 3) where the CO<sub>2</sub> is desuperheated with an air cooler heat exchanger before entering to the condensers (point 4), since generally the discharge temperature is higher than the environment temperature. This cross flow heat exchanger, driven at its nominal speed with a fan of 75 W of power consumption, has a heat transfer area of 0.6 m<sup>2</sup> in the refrigerant side and of 3.36 m<sup>2</sup> in the air side. Next, CO<sub>2</sub> flow is divided and condensated it in two plate heat exchangers (points 5 and 6) with a total heat transfer area of 3.52 m<sup>2</sup>. CO<sub>2</sub> leaving the condensers (points 7 and 8) is joined and its mass flow rate is measured with a Coriolis mass flow meter ( $\dot{m}_r$ ). Then, it enters to the receiver. Following, the refrigerant is subcooled in the IHX (points 9 to 10), which is a brazed plate heat exchanger with a heat transfer area of 0.096 m<sup>2</sup>, and then it feeds the expansion valve of the cycle (point 11), an electronic expansion valve that controls the evaporating

process in a brazed plate evaporator with a heat transfer area of 2.39 m<sup>2</sup>. This valve regulates the degree of superheat at the evaporator exit (point 13) with a NTC and a pressure gauge. Finally, the vapour refrigerant is superheated in the IHX (points 14 to 15). As depicted in Figure 1, the vapour line incorporates a bypass that allows operating with and without the IHX..

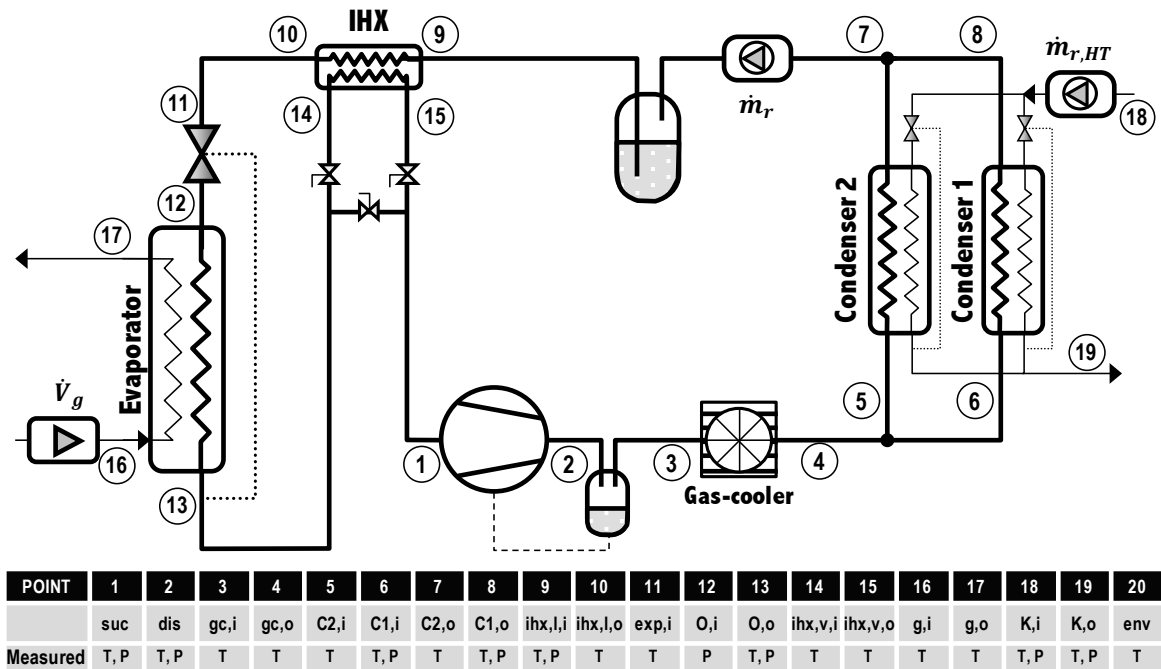


Figure 1. Experimental diagram of the test plant and measurements in each point

For clear understanding of the behaviour of the experimental plant (Figure 1) working with and without the IHX, the operation of the plant at an evaporating temperature of -35 °C, a condensing of -5.6 °C and an environment temperature of 20 °C is presented in a Temperature-Entropy diagram in Figure 2.

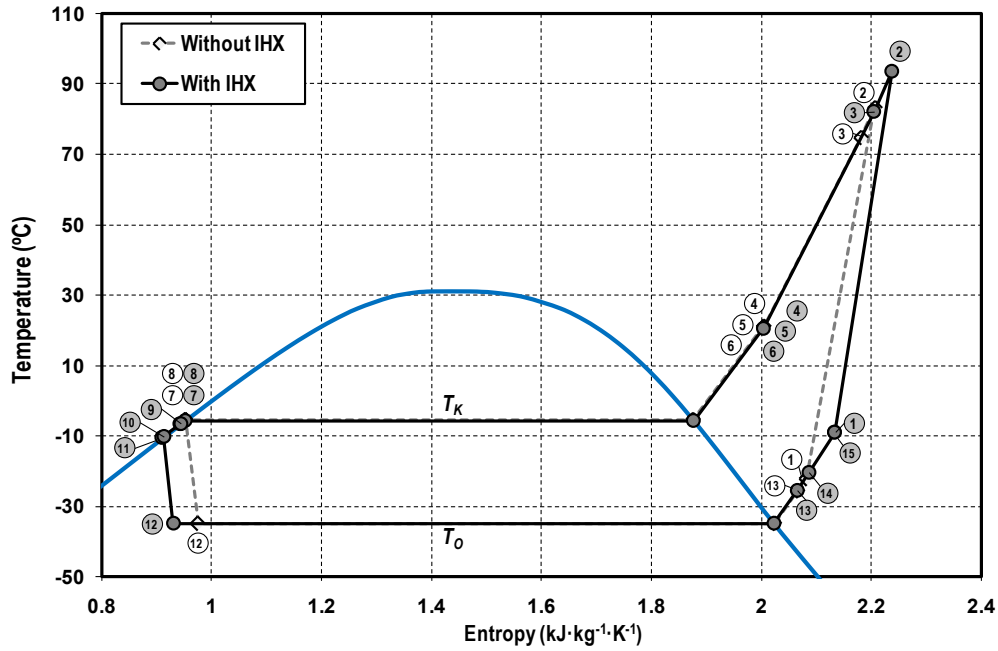


Figure 2. Ts diagram of the plant working with and without IHX ( $T_O = -35\text{ °C}$ ,  $T_K = -5.6\text{ °C}$ )

The heat load to the evaporator is provided with a loop working with a tyfoxit-water mixture (84 % by volume) which allows to operate up to  $-45\text{ °C}$ . This loop allows regulating the inlet temperature of the secondary fluid to the evaporator (point 16) and varying its volumetric flow rate ( $\dot{V}_g$ ). Heat rejection at the condensers is performed through the evaporation of a high-temperature refrigeration cycle which operates with the refrigerant R134a. This evaporation process is controlled in each condenser with individual electronic expansion valves that maintain the degree of superheat of the R134a in  $9\text{ °C}$ , approximately. The refrigerant mass flow rate of the R134a ( $\dot{m}_{r,HT}$ ) is measured with a Coriolis mass flow meter. Speed regulation of the compressor of the R134a cycle is used to modify the condensing conditions of  $\text{CO}_2$ .

The experimental plant is fully instrumented to analyse its energy performance. The location of sensors is presented in Figure 1. It incorporates 19 T-type thermocouples with an uncertainty of  $\pm 0.5\text{ °C}$ , 3 pressure gauges (0-60 bar) for the  $\text{CO}_2$  at low pressure with an uncertainty of  $\pm 0.18\text{ bar}$ , 4 pressure gauges (0-100 bar) for the high pressure of  $\text{CO}_2$  with an uncertainty of  $\pm 0.3\text{ bar}$  and 2 pressure gauges for the R134a (0-10 bar) with a measurement error of  $\pm 0.03\text{ bar}$ . The  $\text{CO}_2$  and R134a coriolis mass flow meters have an uncertainty of  $\pm 0.15\%$  of lecture, and the secondary volumetric flow meter ( $\dot{V}_g$ ) has an uncertainty of  $\pm 0.33\%$ . Power consumption of the compressor is obtained with a digital watt meter with a measurement

error of  $\pm 0.5$  %. All the information obtained from the sensors is gathered by a cRIO data acquisition system (24 bits of resolution) and handled online with an own developed application based on LabView [12].

### 3. Experimental procedure and data validation

---

The test campaign used to evaluate the performance of the subcritical CO<sub>2</sub> refrigeration system working with and without IHX covered evaporating temperatures from -40 to -25 °C and condensing temperatures from -15 to 0.7 °C. The speed of the CO<sub>2</sub> compressor was maintained at its nominal value of 1450 rpm and the test were done fixing a degree of superheat in the CO<sub>2</sub> evaporator of  $9.3 \pm 0.2$  °C, with environmental temperatures of  $20 \pm 3.2$  °C. The fan of the gas-cooler was always kept on, that consuming a constant value of 75 W.

The plant was analysed operating at a fixed evaporating temperature (-40, -35, -30 and -25°C) for different condensing levels, operating with and without the IXH. In total, 38 steady-states of the plant without IHX and 39 with IHX were performed. Each steady-state lasted at least 20 minutes, with 5 seconds sampling rate, with maximum oscillation of the phase-change temperatures of 2 %. Table 1 summarizes the experimental test range evaluation and the variation of the main energy parameters of the plant.

Experimental data was validated comparing the heat transfer rates in the evaporator and in the condenser. In the evaporator, the cooling capacity provided by the cycle, Equation (1), was contrasted with the heat transfer rate of the secondary fluid, Equation (2). Their difference in average was of 2.4 % working without IHX and of 3.3 % with IHX. In the condenser, the heat rejection of CO<sub>2</sub> in the condenser, Equation (3), was compared with the cooling capacity of the R134a cycle, Equation (4). Their difference in average was of 2.7 % working without IHX and of 2.9 % with IHX. To evaluate these heat transfer rates, Tyfoxit properties provided by the manufacturer [13] and Refprop 9.1. [14] database were used for the calculations. The expansion processes were considered isenthalpic. Heat transfer rates validation is presented in Figure 3 for the operation with and without IHX. Also, the uncertainty of the main energy parameters has been evaluated using Moffat's method [15], being the uncertainty of the cooling capacity of 0.675% without IHX and of 0.495% with IHX, and of the COP of 1.103% without IHX and 0.998% with IHX.

$$\dot{Q}_{O,r} = \dot{m}_r \cdot (h_{O,o} - h_{O,i}) \quad (1)$$

$$\dot{Q}_{O,g} = \dot{V}_g \cdot \rho_g \cdot c_{p,g} \cdot (T_{g,i} - T_{g,o}) \quad (2)$$



$$\dot{Q}_{K,r} = \dot{m}_r \cdot \left[ \frac{(h_{C1,i} - h_{C1,o}) + (h_{C2,i} - h_{C2,o})}{2} \right] \quad (3)$$

$$\dot{Q}_{O,HT} = \dot{m}_{r,HT} \cdot (h_{K,o} - h_{K,i}) \quad (4)$$

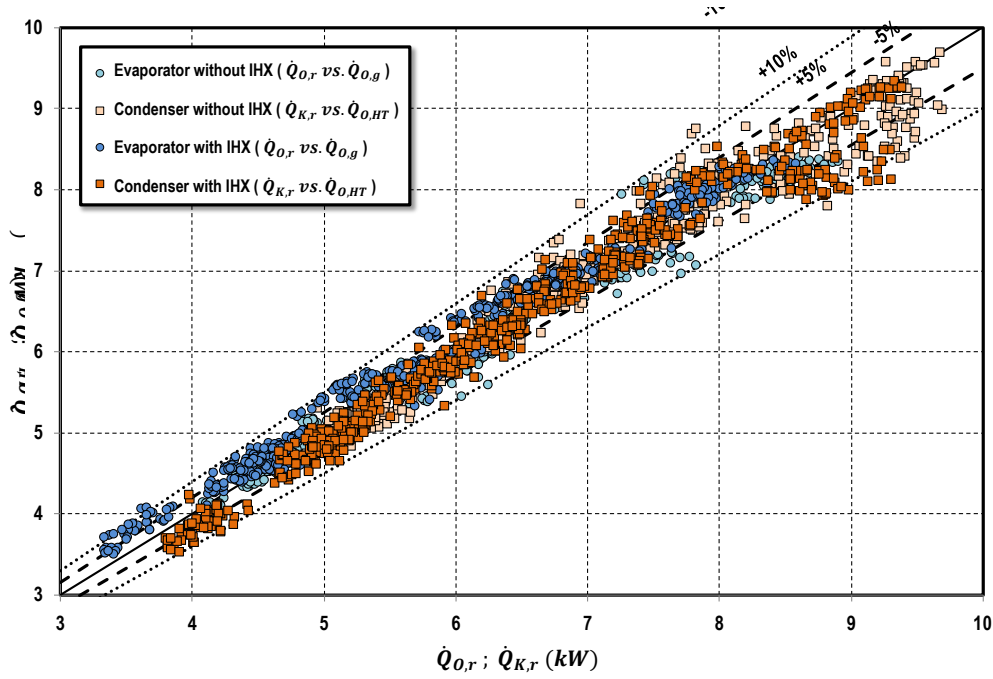


Figure 3. Heat transfer rates validation in condenser and evaporator

## 4. Discussion of experimental results

In this section, we discuss the experimental results of the modifications that implies the use of the IHX in the CO<sub>2</sub> subcritical refrigeration cycle. First, we discuss the thermal effectiveness of the heat exchanger and the modifications it causes on the compressor temperatures, then, we analyse the modifications on the capacity, COP and heat rejection.

### 4.1. Suction and discharge temperatures

The use of the IHX in the refrigeration cycle introduces modifications in the temperature at the inlet of the expansion device and at the compressor suction. These temperature differences, neglecting the superheat

in the evaporator and the subcooling previous entering the IHX, can be related with the thermal effectiveness of the IHX, Equation (5), and evaporation and condensing temperatures, with Equation (6) for the superheating degree, and with Equation (7) for the subcooling degree in the IHX.

$$\varepsilon_{IHX} (\%) = \frac{T_{IHX,v,o} - T_{IHX,v,i}}{T_{IHX,l,i} - T_{IHX,v,i}} \cdot 100 \quad (5)$$

$$SH_{IHX} = T_{IHX,v,o} - T_{IHX,v,i} \cong \varepsilon_{IHX} \cdot (T_K - T_O) \quad (6)$$

$$SUB_{IHX} = T_{IHX,l,i} - T_{IHX,l,o} \cong \varepsilon_{IHX} \cdot (T_K - T_O) \cdot \frac{\bar{c}_{p,v}}{\bar{c}_{p,l}} \quad (7)$$

If Equations (6) and (7) are contrasted, it can be observed that both temperature differences are related between them with the ratio of specific capacities of vapour and liquid. For CO<sub>2</sub>, this ratio ranges from 0.34 to 0.56 in the test range. Accordingly, the superheating degree in the IHX is higher than the subcooling degree, being the first which influences most the behaviour of the plant, since it modifies the suction conditions at the compressor.

Equation (5) was used to determine the experimental thermal effectiveness of the IHX, whose variation range is presented in Table 1, its values ranging from 68.0% to 98.4%. And Equation (8) presents an adjusted polynomial of the measured thermal effectiveness of the IHX as a function of the evaporating and condensing temperatures. In Equation (8) temperatures are expressed in K and presents a maximum uncertainty of 5.36%. The application range of Equation (8) is for evaporating temperatures from -40.00 to -25.00 °C and condensing temperatures from -15.67 to 0.47 °C.

$$\varepsilon_{IHX}(\%) = -1599 - 32.25 \cdot T_K + 0.145 \cdot T_K^2 + 51.56 \cdot T_O - 0.1938 \cdot T_O \cdot T_K \quad (8)$$

From Equation (8) and Table 1, it can be observed that the thermal effectiveness is higher at lower evaporating levels and increases when the condensing temperature rises. Both effects are related with the refrigerant mass flow rate in the cycle, when lowest the refrigerant mass flow rate is, the thermal effectiveness of the subcooler is higher.

This superheating degree in the IHX is translated to the compressor suction temperature. The experimental evolutions of this temperature when the IHX is used and when not are presented in Figure 4. In Figure 4, it is also represented the condition in which the suction temperature equals to the condensing temperature, which would be the situation when the thermal effectiveness of the IHX is of 100%. As it can be observed for the operation without IHX, the suction temperature and the degree of superheat at compressor suction are below the value recommended by the compressor manufacturer (20 °C), which could introduce problems with the lubricating oil. However, the use of the IHX increases this superheating

to admissible values. As it can be observed in Figure 4, the suction temperature when the IHX is used is not much dependent on the evaporating level. The reason of this is that the thermal effectiveness decreases at high evaporating levels but rises at low evaporating temperatures, which is the operating condition when highest superheating degree at suction is needed.

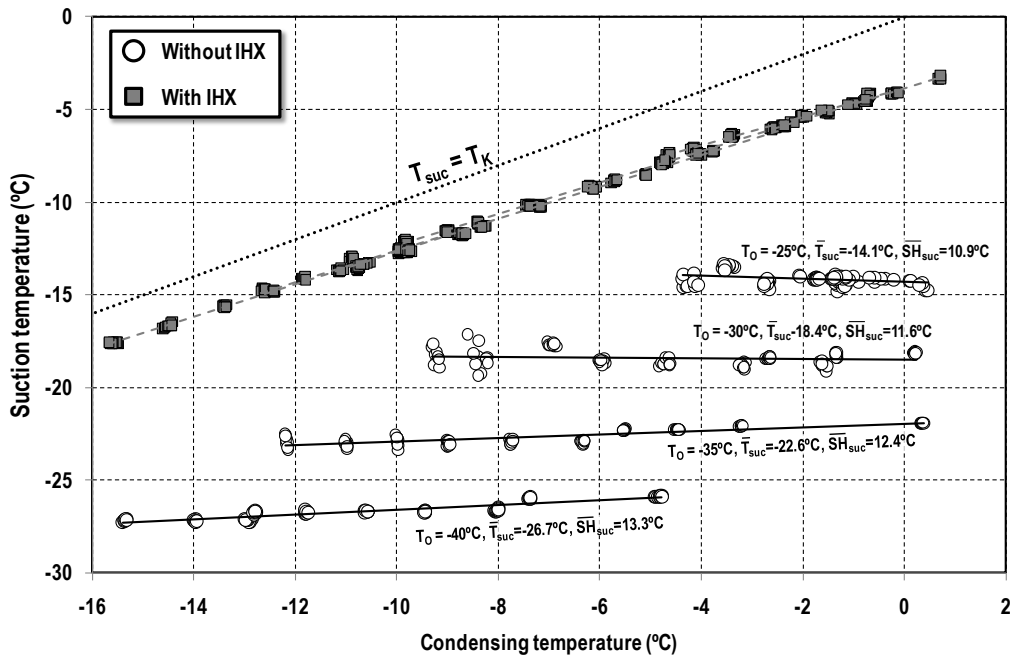


Figure 4. Compressor suction temperature with and without IHX

The superheating degree is directly translated to the compressor discharge temperature. In Figure 5, the experimental discharge temperatures of the CO<sub>2</sub> compressor are presented. The maximum increase of the discharge temperature by the use of the IHX ranged from 10.2 °C at -25.0 °C to 14.7 °C at -40.0 °C. Discharge temperatures are inside the range recommended by the manufacturer and pose no problem, but as it is analysed in subsection 4.5 the increase of this temperature supposes an improvement of the subcritical cycle when it is a part of a cascade system.

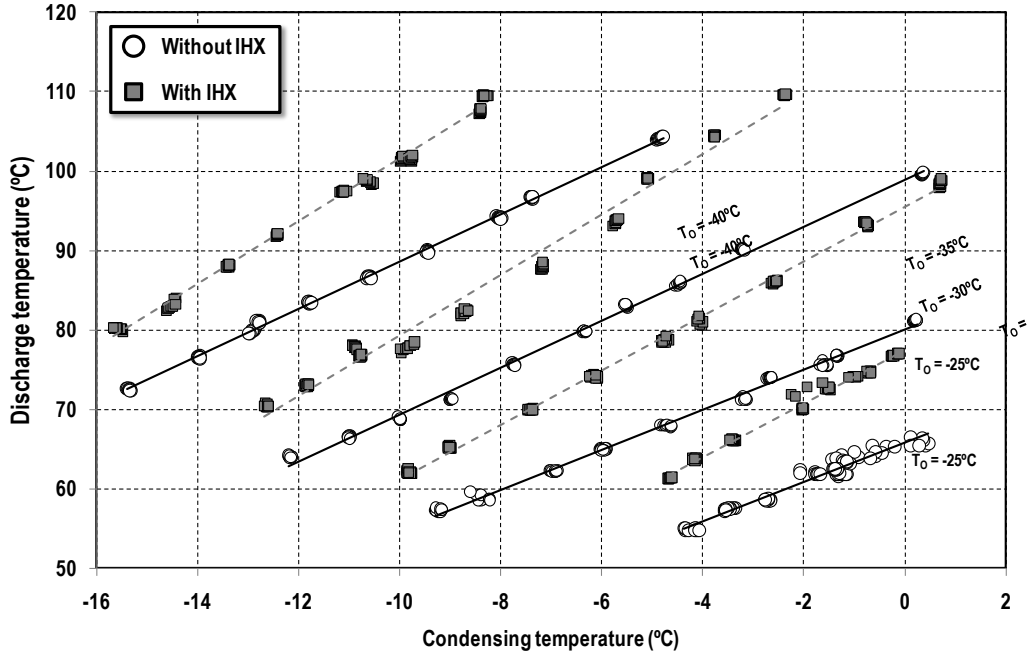


Figure 5. Compressor discharge temperature with and without IHX

## 4.2. Cooling capacity

The IHX has two opposite effects on the refrigeration capacity of the cycle, Equation (9): First, the increase of the suction temperature causes an increment of the specific suction volume, whose consequence is a reduction of the refrigerant mass flow rate, Equation (10), which tends to reduce the refrigeration capacity. Second, the subcooling in the IHX increases the specific cooling capacity, which tends to increase the refrigeration capacity of the cycle. The variation of the refrigeration capacity will depend on both effects.

$$\dot{Q}_{O,r} = \dot{m}_r \cdot q_o \quad (9)$$

$$\dot{m}_r = \frac{\eta_v}{v_{suc}} \cdot \dot{V}_G \quad (10)$$

Regarding the modification of mass flow rate, their experimental evolutions with and without the IHX are represented in Figure 6. It can be observed the use of the IHX always reduces the refrigerant mass flow rate. This reduction varies between 3.83 to 5.5 % at -25 °C and 3.70 to 5.76 % at -40 °C. The main reason of this reduction is the increase of the specific suction volume, since the volumetric efficiency of the compressor is not modified according to experimental data.

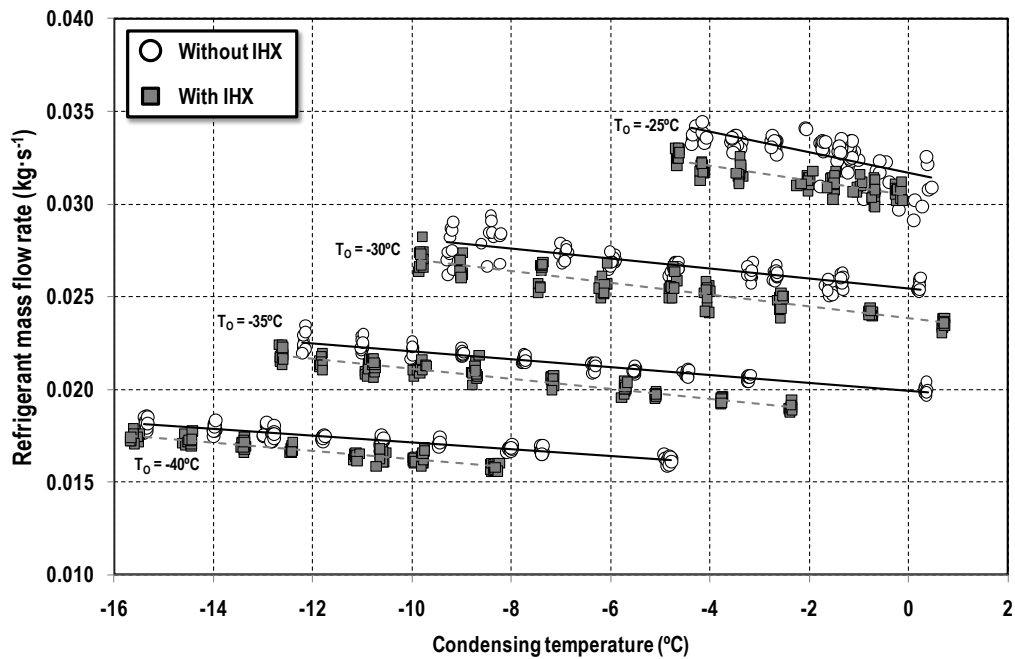


Figure 6. Refrigerant mass flow rate with and without IHX

On the other side, the experimental specific cooling capacities are represented in Figure 7 for the operation with and without IHX. As it can be observed, the specific cooling capacity is always increased due to the subcooling of the liquid in this heat exchanger. Inside the test range, the increase of the specific cooling capacities vary between 2.0 to 2.8 % at -25 °C and 3.2 to 5.3 % at -40 °C. It needs to be mentioned that the increase of the specific capacity is higher at high condensing temperatures.

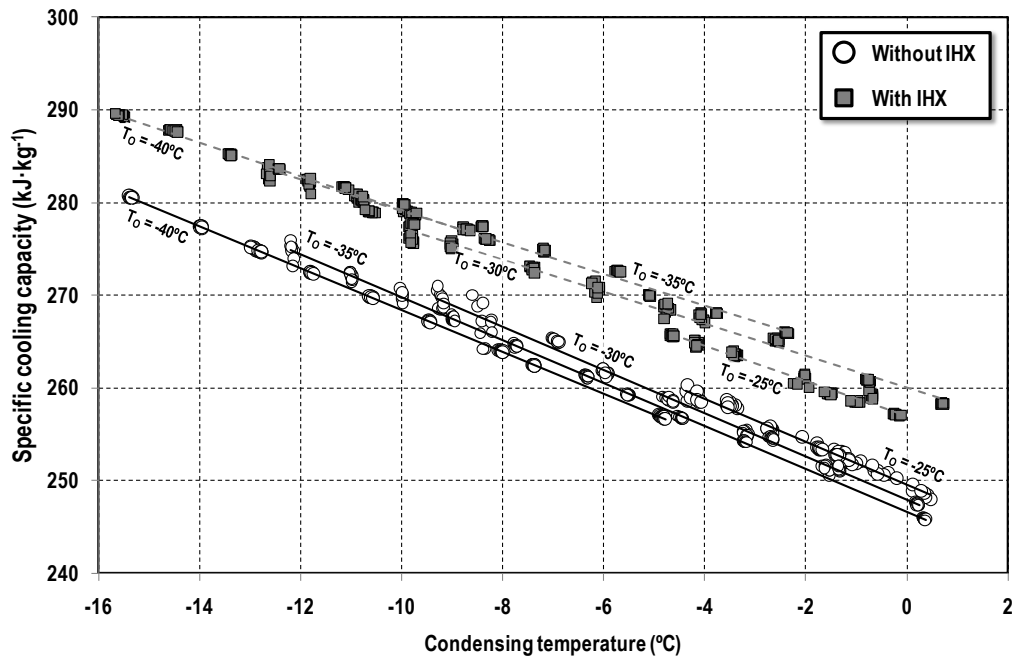


Figure 7. Specific cooling capacity with and without IHX

And finally, the combination of the above mentioned effects is presented in Figure 8. As it can be observed, the effect of reduction of refrigerant mass flow rate overcomes the increase of specific cooling capacity, resulting in a decrease of capacity in all the measured range. The reductions of capacity vary between 1.1 to 3.7 % at -25 °C and 1.6 to 3.5 % at -40 °C. This evolution of the capacity in CO<sub>2</sub> subcritical plants is different from the observed in CO<sub>2</sub> transcritical cycles, where the use of the IHX provides increases of capacity up to 12 % [8]. In this case, although the reductions on capacity are small, the strongest are at high evaporating temperatures.

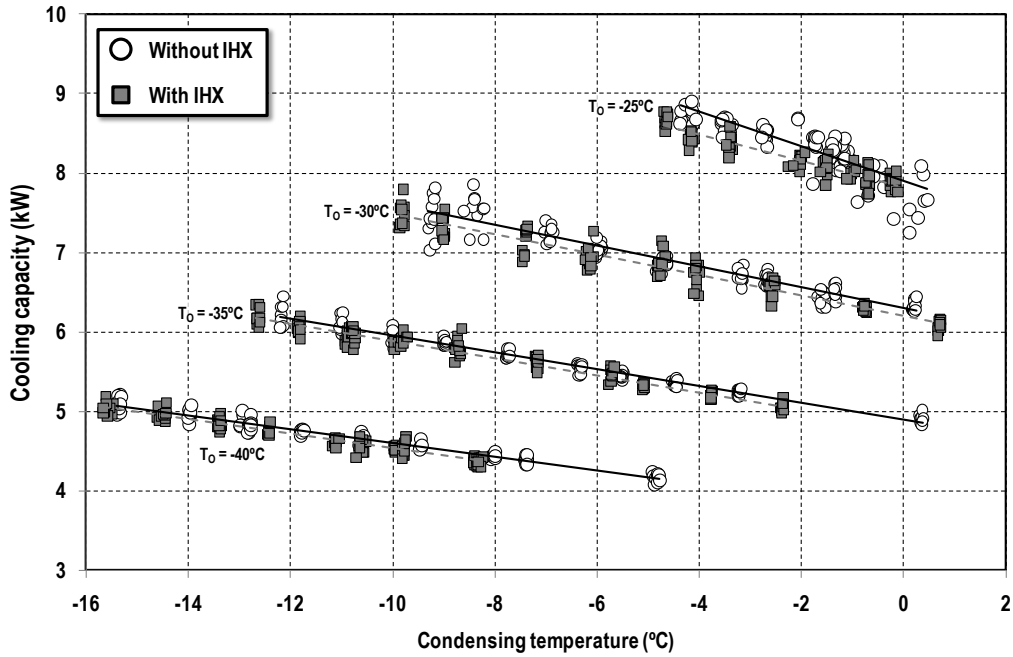


Figure 8. Cooling capacity with and without IHX

### 4.3. COP

The next energy parameter in importance to be analysed is the COP of the plant and its variations when the IHX is used. The COP depends on the cooling capacity, the compressor power consumption and the power consumption of the fan of the gas-cooler, as presented by Equation (11).

$$COP = \frac{\dot{Q}_{o,r}}{P_C + P_{gc}} \quad (11)$$

About the power consumption, the power consumption of the fan of the gas-cooler has a constant value of 75W, whereas the variations of the compressor power consumption are for all the tests below 0.5 %, in the same way as analysed for transcritical CO<sub>2</sub> plants [8]. Accordingly, variations of COP are more bonded to variations of capacity.

The COP experimental evolutions over the test range are presented in Figure 9. As it can be observed the reductions on COP when the IHX is used are small and they can be also positive at low evaporating temperatures and low condensing temperatures. For the experimental data, the reductions in COP vary from 1.58 to 3.29 % at -25 °C and from 1.06 to an increase of 0.45 % at -40°C.

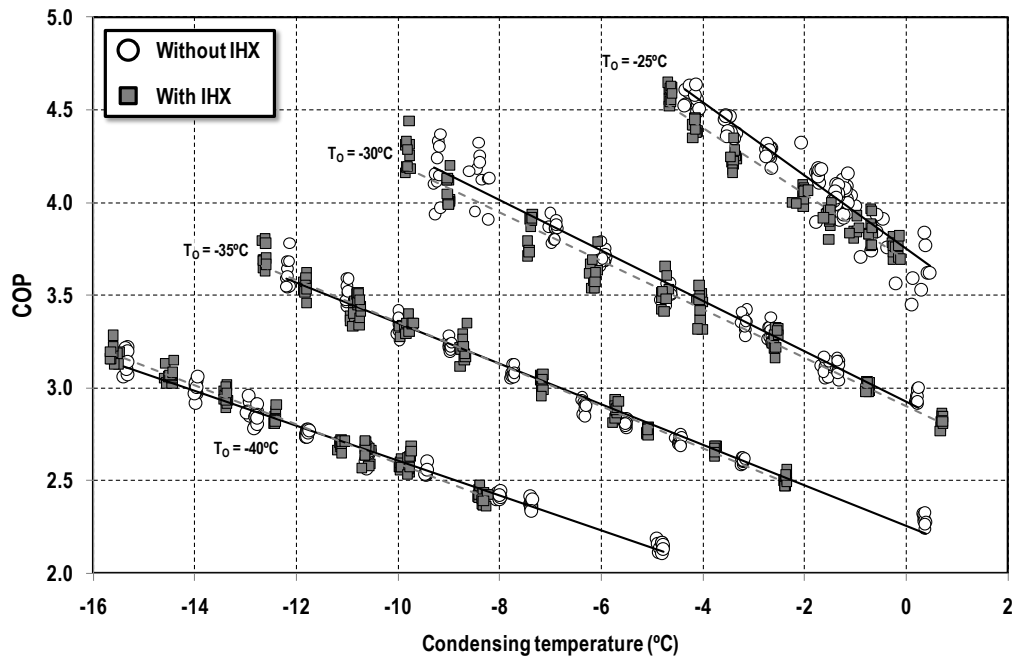


Figure 9. COP with and without IHX

#### 4.4. Heat rejection

Finally, although not usually considered in works related with the performance of the IHX, it is worth analysing the variations on the heat rejection induced by the use of this heat exchanger. As presented in Figure 5, the compressor discharge temperatures are always higher than the environment temperature ( $20 \pm 3.2$  °C). Due to this reason, this refrigeration plant incorporates a gas-cooler heat exchanger previous entering the condensers of the plant (Figure 1) to reject the possible heat to the environment (points 3 to 4 in Figure 1) and avoid pumping it to the high temperature cycle. Accordingly, the heat transfer we analyse is the sum of the heat transferred to the environment in the gas-cooler and the heat transfer during condensation of CO<sub>2</sub> in the condensers.

In Figure 10, the heat rejection in the gas-cooler and in the condensers is presented, this evaluated with Equation (12). This heat rejection would be the one to be transferred to the high-temperature cycle if the gas-cooler is not used. In this case, the use of the IHX produces a reduction of this heat transfer, caused by the reduction of the refrigerant mass flow rate (Figure 6) but attenuated by the increase of the compressor discharge temperature (Figure 5). The measured reductions of this heat transfer rate vary from 0.77 to 3.41 % at -25 °C and 2.12 to 2.45 % at -40 °C. Since over all the operating range this heat



transfer rate is reduced, it corresponds to a beneficial effect of the IHX, since the high temperature cycle would have less load to be absorbed.

$$\dot{Q}_{K,r} + \dot{Q}_{gc,r} = \dot{m}_r \cdot \left[ h_{gc,i} - \frac{h_{C1,o} + h_{C2,o}}{2} \right] \quad (12)$$

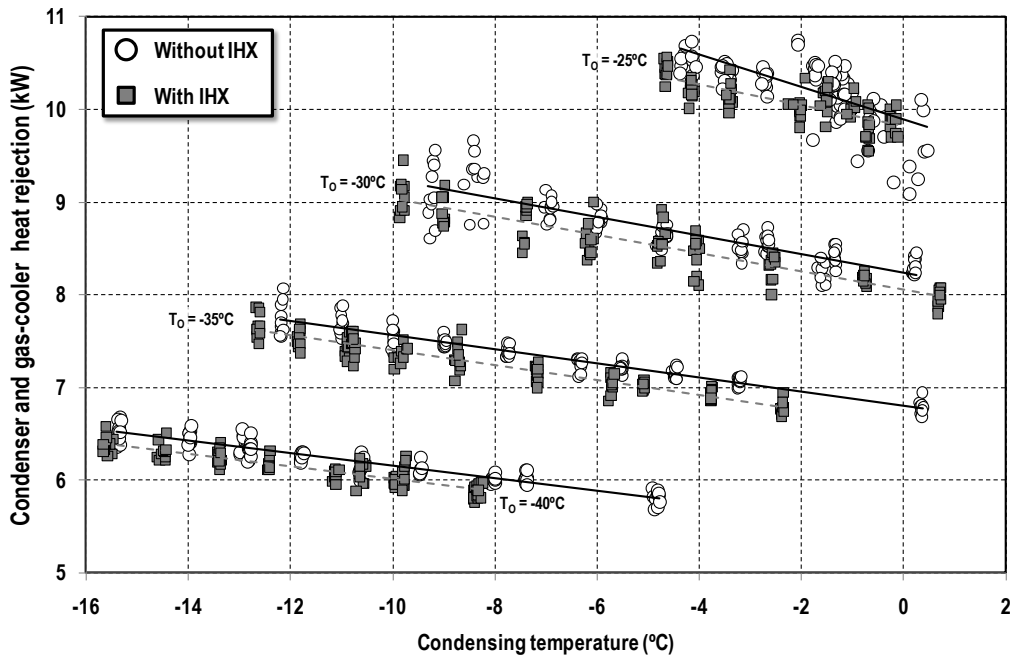


Figure 10. Condenser and gas-cooler heat rejection with and without IHX

Considering only the heat rejection at the condenser, this evaluated from experimental data with Equation (3), its evolutions are presented in Figure 11. Again, the use of the IHX reduces the heat to be transferred in the condensers, in this case because of the reduction of the refrigerant mass flow rate, since the inlet temperature of the refrigerant to the condensers (points 5 and 6) practically coincide for the operation with and without IHX, as it can be appreciated in Figure 2. This coincidence of the inlet temperature to the condensers is caused by the gas-cooler. In this case, the reductions of the condensing heat transfer vary from 4.78 to 4.91 % at -25 °C and from 3.71 to 4.82 % at -40 °C.

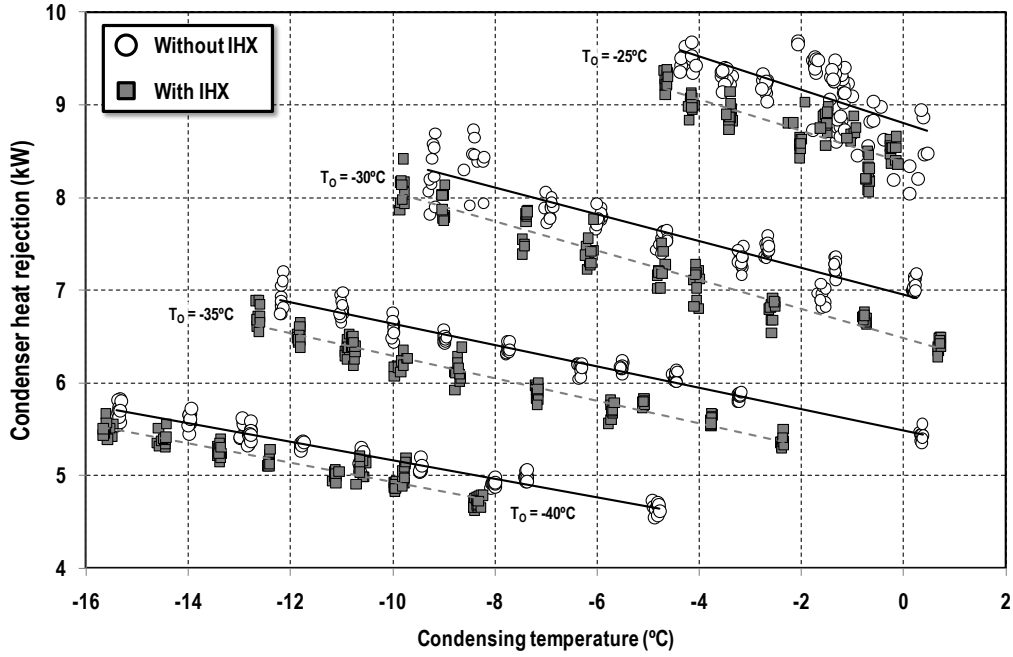


Figure 11. Condenser heat rejection with and without IHX

#### 4.5. Effect on a cascade system

As mentioned before, the use of the IHX with the combination of a gas-cooler in the subcritical cycle reduces the heat to be transferred to the high temperature cycle. To analyse the effect of the IHX on the whole cycle, that is a combination of the subcritical cycle with a high temperature cycle (cascade refrigeration system), the COP of the whole system must be considered.

The COP of the cycle combinations, denoted as  $COP_{casc}$ , is expressed by Equation (13), being it obtained dividing the cooling capacity provided by the subcritical cycle ( $\dot{Q}_{O,r}$ ) by the power consumption of the subcritical compressor ( $P_C$ ) and of the gas-cooler ( $P_{gc}$ ) of the subcritical cycle and the power consumption of the high temperature cycle ( $P_{C,HT}$ ). This last can be related with the  $COP_{HT}$  of the high temperature cycle with Equation (14), where it is considered that the condensation heat transfer of the subcritical cycle ( $\dot{Q}_{K,r}$ ) is equal to the refrigeration load of the high temperature cycle. The combination of Equations (13) and (14) results in Equation (15). If Equation (15) is analysed, considering the  $COP_{HT}$  constant, it can be observed that the  $COP_{casc}$  would be improved if  $\dot{Q}_{K,r}$  is reduced.

$$COP_{casc} = \frac{\dot{Q}_{O,r}}{P_C + P_{gc} + P_{C,HT}} \quad (13)$$

$$P_{C,HT} = \frac{\dot{Q}_{K,r}}{COP_{HT}} \quad (14)$$

$$COP_{casc} = \frac{\dot{Q}_{O,r}}{P_C + P_{gc} + \frac{\dot{Q}_{K,r}}{COP_{HT}}} \quad (15)$$

To quantify the effect of the IHX on the cascade system, the percentage variation of the  $COP_{casc}$  when using the IHX is evaluated with Equation (16), where the  $COP_{casc}$  is obtained with Equation (15). To evaluate  $COP_{casc}$ , the presented experimental data of the  $CO_2$  cycle was used. For the evaluation, it was considered a constant temperature difference in the cascade heat exchanger of  $3^\circ C$ , corresponding to an average value obtained from the experimental evaluation of a R134a/ $CO_2$  cascade plant [16], and a linear dependent  $COP_{HT}$  relation for the high temperature cycle ( $COP_{HT}=2.5-0.05151 \cdot T_{O,HT}$ ), in this case, also obtained from the experimental R134a/ $CO_2$  cascade plant [16] for a constant condensing temperature of the high temperature cycle of  $40^\circ C$ .

$$\Delta COP_{casc} = \frac{COP_{casc}^{IHX} - COP_{casc}}{COP_{casc}} \cdot 100 \quad (16)$$

Accordingly, in Figure 12 the  $COP_{casc}$  modifications of the cascade cycle due to the use of the IHX in the  $CO_2$  cycle are presented for different evaporating levels, different low temperature condensing temperatures ( $T_K$  in Figure 12) at a constant condensing temperature of the high temperature cycle ( $T_{K,HT}=40^\circ C$ ). As it can be observed in Figure 12, the use of the IHX has a positive effect on the COP of the cascade plant, ranging the improvements between 0.15 to 2.91 %. It can be observed that the improvements are higher at lower evaporating temperatures, especially at  $-40$  and  $-35^\circ C$ , where the IHX is more necessary, and thus, more convenient.

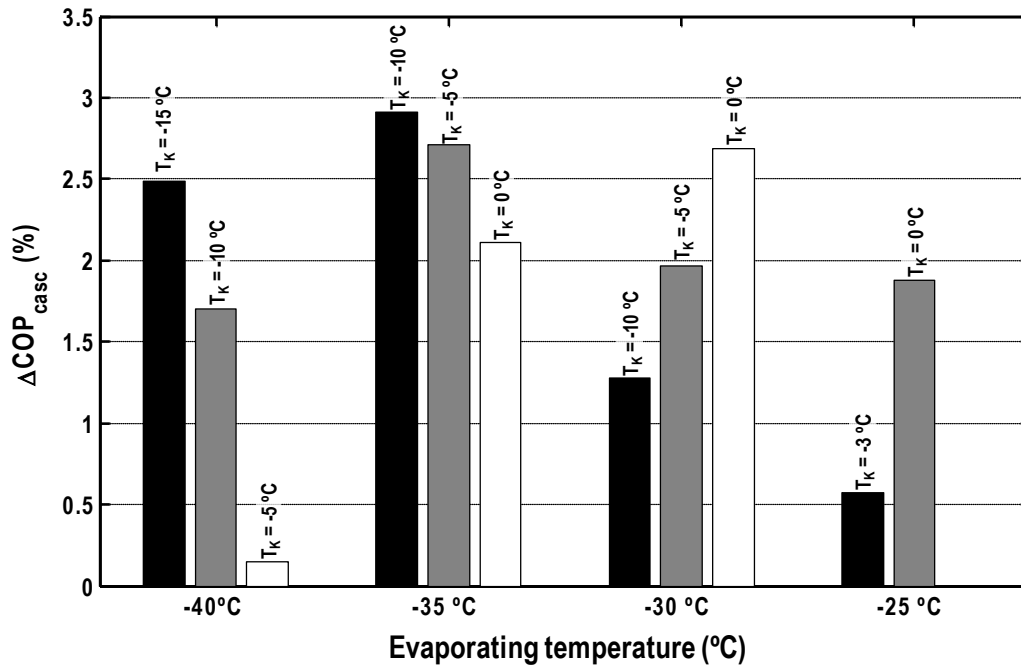


Figure 12. Variation of the COP of the cascade system with the use of the IHX ( $T_{K,HT}=40^\circ\text{C}$ )

## 5. Conclusions

In this work the effect of the Internal Heat Exchanger (IHX) in a  $\text{CO}_2$  subcritical refrigeration cycle has been analysed from an experimental point of view. The evaluation has been performed with a subcritical single-stage  $\text{CO}_2$  cycle driven by a semi hermetic compressor with a refrigeration plant that incorporates a gas-cooler previous entering the condensers. The experimental evaluation has covered evaporating temperatures from  $-40$  to  $-25$  °C and condensing temperatures from  $-15$  to  $0$  °C, the usual temperature range in commercial refrigeration.

It has been observed that the IHX operated with high thermal effectiveness, those ranging from 68.0 to 98.4 %, being its effectiveness higher at lower evaporating levels. This dependence of the effectiveness on the evaporating level resulted in compressor suction temperatures independent on the evaporating level, assuring in all the evaluation range a degree of superheat at suction higher than  $20$  °C. The maximum measured discharge temperature increment were of  $14.7$  °C, and occurred at low evaporating levels.

Regarding the effect of the IHX on the energy parameters of the subcritical cycle, it has been observed a reduction of the capacity provided by the plant, which ranged from 1.1 to 3.7 %. This reduction was mainly

induced by the reduction of the refrigerant mass flow rate through the CO<sub>2</sub> cycle. About the effect on the COP of the CO<sub>2</sub> cycle, reductions from 1.8 to 3.29 % were measured at -25 °C of evaporation temperature, but small improvements up to 0.45 % were observed at -40 °C.

Nonetheless, the use of the IHX with a combination of a gas-cooler in the CO<sub>2</sub> subcritical cycle resulted in reductions of the heat to be transferred in the cascade condenser, reductions which were more important at low evaporating levels. This reductions of the heat transferred to the high temperature cycle in cascade systems produced increments on the COP of the cascade system from 0.15 to 2.91 %.

Accordingly, it can be concluded that despite the reductions of capacity and COP in the CO<sub>2</sub> subcritical cycle, the use of an IHX in the CO<sub>2</sub> cycle introduces beneficial effects, since it assures a minimum degree of superheat at the suction of the compressor, allows avoiding problems with the lubricant oil and can increment the COP of the whole cascade system.

## **6. Acknowledgements**

---

The authors gratefully acknowledge Jaume I University of Spain, who financed the present study through the research project P1·B2013-10.

## 7. References

---

- [1] E. Granryd, I. Ekroth, P. Lundqvist, A. Melinder, B. Palm, P. Rohlin, Refrigerating Engineering, Royal Institute of Technology, KTH, Department of Energy Technology, Division of Applied Thermodynamics and Refrigeration, 2009.
- [2] P.A. Domanski, D.A. Didion, J.P. Doyle, Evaluation of suction-line/liquid-line heat exchange in the refrigeration cycle, *International Journal of Refrigeration*, 17 (1994) 487-493.
- [3] R. Mastrullo, A.W. Mauro, S. Tino, G.P. Vanoli, A chart for predicting the possible advantage of adopting a suction/liquid heat exchanger in refrigerating system, *Applied Thermal Engineering*, 27 (2007) 2443-2448.
- [4] European Commission, Regulation (EU) No 517/2014 of the European Parliament and of the Council of 16 April 2014 on fluorinated greenhouse gases and repealing Regulation (EC) No 842/2006., (2014).
- [5] A. da Silva, E.P. Bandarra Filho, A.H.P. Antunes, Comparison of a R744 cascade refrigeration system with R404A and R22 conventional systems for supermarkets, *Applied Thermal Engineering*, 41 (2012) 30-35.
- [6] J.A. Dopazo, J. Fernández-Seara, Experimental evaluation of a cascade refrigeration system prototype with CO<sub>2</sub> and NH<sub>3</sub> for freezing process applications, *International Journal of Refrigeration*, 34 (2011) 257-267.
- [7] F.Z. Zhang, P.X. Jiang, Y.S. Lin, Y.W. Zhang, Efficiencies of subcritical and transcritical CO<sub>2</sub> inverse cycles with and without an internal heat exchanger, *Applied Thermal Engineering*, 31 (2011) 432-438.
- [8] E. Torrella, D. Sánchez, R. Llopis, R. Cabello, Energetic evaluation of an internal heat exchanger in a CO<sub>2</sub> transcritical refrigeration plant using experimental data, *International Journal of Refrigeration*, 34 (2011) 40-49.
- [9] D. Sánchez, J. Patiño, R. Llopis, R. Cabello, E. Torrella, F.V. Fuentes, New positions for an internal heat exchanger in a CO<sub>2</sub> supercritical refrigeration plant. Experimental analysis and energetic evaluation, *Applied Thermal Engineering*, 63 (2014) 129-139.
- [10] C. Aprea, M. Ascani, F. De Rossi, A criterion for predicting the possible advantage of adopting a suction/liquid heat exchanger in refrigerating system, *Applied Thermal Engineering*, 19 (1999) 329-336.
- [11] S.A. Klein, D.T. Reindl, K. Brownell, Refrigeration system performance using liquid-suction heat exchangers, *International Journal of Refrigeration*, 23 (2000) 588-596.

- [12] R. Cabello, R. Llopis, D. Sánchez, E. Torrella, REFLAB: An interactive tool for supporting practical learning in the educational field of refrigeration, *International Journal of Engineering Education*, 27 (2011) 909-918.
- [13] TYFO, High-performance low viscous secondary refrigerant for applications down to -55°C. In: [www.tyfo.de/uploads/TI/IT-TYFOXIT-F15-F50\\_es\\_2013.pdf](http://www.tyfo.de/uploads/TI/IT-TYFOXIT-F15-F50_es_2013.pdf) (29/06/2014), in, 2013.
- [14] E.W. Lemmon, M.L. Huber, M.O. McLinden, REFPROP, NIST Standard Reference Database 23, v.9.1. National Institute of Standards, Gaithersburg, MD, U.S.A., (2013).
- [15] R.J. Moffat, Using Uncertainty Analysis in the Planning of an Experiment, *Journal of Fluids Engineering*, 107 (1985) 173-178.
- [16] C. Sanz-Kock, R. Llopis, D. Sánchez, R. Cabello, E. Torrella, Experimental evaluation of a R134a/CO<sub>2</sub> cascade refrigeration plant, *Applied Thermal Engineering*, 73 (2014) 39-48.

## TABLES

Operation with IHX												
$T_o$ (°C)	$\sigma(T_o)$ (°C)	$T_k$ (°C)	SH (°C)	$\epsilon_{IHX}$ (%)	$m_r$ (kg·s <sup>-1</sup> )	$Q_{o,r}$ (W)	$P_c$ (W)	$Q_{K,r}$ (W)	$Q_{gc,r}$ (W)	$Q_{IHX}$ (W)	COP	tests
-25.00	0.06	-4.70 to -0.11	9.08	68.0 to 79.5	0.030 to 0.033	7735 to 8776	1810 to 2029	8065 to 9383	1143 to 1556	199 to 289	3.69 to 4.65	8
-30.01	0.10	-9.86 to -0.73	9.31	77.4 to 94.0	0.024 to 0.028	6240 to 7792	1678 to 2036	6541 to 8419	968 to 1546	146 to 287	2.98 to 4.44	9
-34.93	0.12	-12.67 to -5.67	9.44	86.9 to 96.8	0.020 to 0.022	5333 to 6350	1593 to 1826	5564 to 6889	924 to 1358	149 to 260	2.81 to 3.80	11
-40.00	0.07	-15.67 to -8.39	9.33	82.8 to 98.4	0.016 to 0.018	4321 to 5188	1503 to 1727	4623 to 5665	864 to 1172	144 to 204	2.41 to 3.28	10
Operation without IHX												
-25.00	0.14	-4.37 to 0.47	9.15	-	0.029 to 0.034	7253 to 8901	1831 to 2042	8045 to 9688	944 to 1311	-	3.45 to 4.64	9
-30.05	0.13	-9.30 to -1.53	9.37	-	0.025 to 0.029	6302 to 7851	1706 to 1995	6816 to 8733	789 to 1333	-	3.05 to 4.37	10
-35.02	0.07	-12.20 to -4.42	9.28	-	0.021 to 0.023	5302 to 6449	1631 to 1901	6006 to 7202	812 to 1107	-	2.69 to 3.78	10
-40.04	0.05	-15.40 to -7.99	9.35	-	0.017 to 0.019	4394 to 5210	1540 to 1764	4865 to 5823	811 to 1108	-	2.40 to 3.22	10

Table 1. Experimental test range